

Iron Line Spectroscopy of NGC 4593 with *XMM-Newton*: Where is the Black Hole Accretion Disk?

Christopher S. Reynolds¹, Laura W. Brenneman¹, Jörn Wilms^{2,3}, and Mary Elizabeth Kaiser⁴

¹Dept. of Astronomy, University of Maryland, College Park, MD 20742, USA.

²Institut für Astronomie und Astrophysik, Abt. Astronomie, Universität Tübingen, Sand 1, 72076 Tübingen, Germany

³Department of Physics, University of Warwick, Coventry, CV4 7AL

⁴Dept. of Physics and Astronomy, Johns Hopkins University, 3400 Charles Street, Baltimore, MD 21218.

In press

ABSTRACT

We present an analysis of the 2–10 keV *XMM-Newton*/EPIC-pn spectrum of the Seyfert-1 galaxy NGC 4593. Apart from the presence of two narrow emission lines corresponding to the K α lines of cold and hydrogen-like iron, this spectrum possesses a power-law form to within $\sim 3 - 5\%$. There is a marked lack of spectral features from the relativistic regions of the black hole accretion disk. We show that the data are, however, consistent with the presence of a radiatively-efficient accretion disk extending right down to the radius of marginal stability if it possesses low iron abundance, an appropriately ionized surface, a very high inclination, or a very centrally concentrated emission pattern (as has been observed during the Deep Minimum State of the Seyfert galaxy MCG-6-30-15). Deeper observations of this source are required in order to validate or reject these models.

Key words: accretion, accretion disks – black hole physics – galaxies:individual(NGC4593) – galaxies:Seyferts

1 INTRODUCTION

The fluorescent K α emission line of iron is currently the best probe we have to study strong-field gravitational effects in the vicinity of black holes. This line, together with an associated backscattered continuum, is readily formed when a hard X-ray continuum source irradiates the surface of a relatively cold and optically-thick slab of gas (Basko 1978; Guilbert & Rees 1988; Lightman & White 1988; George & Fabian 1991; Matt et al. 1991). Nowadays, the hard X-ray source is usually identified with thermal Comptonization from an accretion disk corona, and the optically-thick structure as the accretion disk itself (see Reynolds & Nowak 2003 for a recent review). The diagnostic power of these spectral features lies in investigations of their Doppler broadening and gravitational redshifting (Fabian et al. 1989; Laor 1991). The best example to date of using these features to probe strong-field gravity is the Seyfert-1.2 galaxy MCG-6-30-15 (Tanaka et al. 1995; Wilms et al. 2001; Fabian et al. 2002; Reynolds et al. 2004). This object displays a highly-broadened and skewed iron line that is strongly suggestive of emission from an accretion disk reaching down to near the radius of marginal stability for a rapidly-rotating black hole. As yet, there is

no competing model that can explain, in detail, the iron line feature in MCG-6-30-15.

However, it is an open question whether these relativistic spectral features are generic in the spectra of various classes of active galactic nuclei (AGN). Nandra et al. (1997a) used data from the *ASCA* observatory to conclude that relativistically-broadened iron lines are very common features in the X-ray spectra of Seyfert-1 nuclei. On the other hand, *ASCA* found that these emission lines were often weaker and/or narrower in the X-ray spectra of low-luminosity AGN (e.g., Reynolds, Nowak & Maloney 2000; Terashima et al. 2002), high-luminosity AGN (Nandra et al. 1997b) and radio-loud AGN (Sambruna, Eracleous & Mushotzky 1999).

Recent results from the European Photon Imaging Camera (EPIC) on board the *XMM-Newton* observatory have painted a more complex picture. While *XMM-Newton* has, indeed, found undisputed cases of broad iron lines in the Seyfert galaxies MCG-6-30-15 (Wilms et al. 2001, Fabian et al. 2002), MCG-5-23-16 (Dewangan, Griffiths & Schurch 2003), NGC 3516 (Turner et al. 2002), Mrk335 (Gondoin et al. 2002), and Mrk766 (Pounds et al. 2003a), other Seyfert-1 galaxies appear to show an absence of such features, with the best example to date being NGC 5548 (Pounds et al.

2003b). Clearly, the presence or absence of a relativistic iron line depends upon currently unknown factors and is not a simple function of AGN class.

Progress must be made by careful analysis of as many AGN X-ray spectra as possible. With this motivation, this *Paper* presents a careful analysis of the hard-band *XMM-Newton* EPIC-pn spectrum of the Seyfert-1 galaxy NGC 4593 ($z = 0.009$). Section 2 describes in brief our observation and data reduction techniques. Section 3 presents an analysis of the 2–10 keV spectrum of NGC 4593 and demonstrates a marked absence of a “standard” relativistic iron line, a result which is discussed in more detail in Section 4. Section 5 summarizes our principal conclusions.

2 OBSERVATIONS AND DATA REDUCTION

XMM-Newton observed NGC 4593 for a total of 76 ksec during orbit 465. All instruments were operating during this observation. The EPIC-pn was operated in its small-window mode to prevent photon pile-up, using the medium-thick filter to avoid optical light contamination. The EPIC MOS-1 camera took data in the fast uncompressed timing mode, and the MOS-2 camera operated in prime partial W2 imaging mode. Though the MOS results will not be discussed further here, they mirrored the pn data within the expected errors of calibration effects. The average count rate for the pn instrument was 29.78 ct s^{-1} .

The pipeline data were reprocessed using version 5.4.1 of the Science Analysis Software, and the matching calibration files (CCF from 2003 January 14 via <http://xmm.vilspa.esa.es/ccf>). From these, we rebuilt the calibration index file using `cifbuild`, and then reprocessed the EPIC data using the `emproc` and `epproc` tasks. Bad pixels and cosmic ray spikes (narrow time filtering) were removed from the events files via the `evselect` task within the SAS. Circular extraction regions 40 arcsecs in radius were then defined both on and off the source for generating source and background spectra, respectively, using the `xmmselect` task. Response matrices and ancillary response files were created using `rmfgen` and `arfgen`, and the data were then grouped with their respective response files using the `grppha` such as to impose a minimum of 25 counts per spectral bin. This binning is required in order to get sufficient counts per bin to make χ^2 -spectral fitting a valid statistical process. Spectral modeling and analysis was performed using the XSPEC package.

3 THE 2–10 KEV EPIC-PN SPECTRUM

In this paper, we analyze only the hard band (2–10 keV) data from the EPIC-pn camera. This energy restriction prevents us from having to model the soft excess, ionized absorption, and recombination line emission present in the 0.5–2 keV band. The soft spectrum of this object will be discussed in detail in another publication (Brenneman et al. 2004).

Initially, we fit this spectrum with a model consisting of a simple power-law modified by neutral Galactic absorption with a column density of $N_{\text{H}} = 1.97 \times 10^{20} \text{ cm}^{-2}$ (Elvis, Wilkes & Lockman 1989). The best fitting power-law index is $\Gamma = 1.69 \pm 0.01$ ($\chi^2/\text{dof} = 1993/1476$) giving a model

2–10 keV flux and luminosity of $4.41 \times 10^{-11} \text{ erg cm}^{-2} \text{ s}^{-1}$ and $7.60 \times 10^{42} \text{ erg s}^{-1}$, respectively. This best-fit is shown in Fig.1a. The power-law describes the spectrum well apart from two obvious line-like features between 6–7 keV. Modeling these features with two Gaussian profiles improves the overall fit significantly ($\chi^2/\text{dof} = 1526/1470$). Best-fitting (rest-frame) centroid energies, standard deviations and equivalent widths for these two features are; $E_1 = 6.39 \pm 0.01 \text{ keV}$, $\sigma_1 = 86 \pm 17 \text{ eV}$, $\text{EW}_1 = 117 \pm 11 \text{ eV}$ and $E_2 = 6.95 \pm 0.05 \text{ keV}$, $\sigma_2 = 102_{-79}^{+94} \text{ eV}$, $\text{EW}_2 = 39 \pm 13 \text{ eV}$. It seems very likely that these features are the K α emission lines of “cold” iron (i.e., less than FeXVII) and hydrogen-like iron that are expected at 6.40 keV and 6.97 keV, respectively. We do not detect a helium-like iron line at 6.67 keV — the upper limit to the equivalent width of any such line is $\text{EW} < 13 \text{ eV}$.

3.1 The narrow emission lines

These relatively narrow emission lines likely originate from material that is rather distant from the central black hole. The cold iron line is centered on the systemic velocity of NGC 4593 and is well resolved ($\text{FWHM}=10900 \pm 2200 \text{ km s}^{-1}$). For comparison, the broad optical H β line in NGC 4593 has $\text{FWHM}=4910 \pm 300 \text{ km s}^{-1}$ (Grupe et al. 2004), approximately half of the velocity width of the cold iron line. Thus, it seems clear that the cold iron line is originating from a region that lies significantly inside of the optical broad emission line region (OBLR), and hence cannot be identified with X-ray reflection from the classic “molecular gas torus” postulated by unified Seyfert schemes. We note that the *XMM-Newton* data sets no useful constraints on the presence of a Compton backscattered continuum expected from X-ray reflection by cold matter, thus the possibility remains that this line might be formed by the X-ray illumination and subsequent fluorescence of optically-thin material (as opposed to the optically-thick material normally envisaged in X-ray reflection).

The hydrogen-like iron line, on the other hand, is only marginally resolved ($\text{FWHM}=12200_{-9400}^{+11200} \text{ km s}^{-1}$). Thus, it is not possible to conclude where, relative to the OBLR, the ionized emission originates. It is, however, possible to say something about the physical process underlying this emission. If one supposes that this line is emitted by collisionally-ionized thermal plasma (described by the `mekal` model in XSPEC; Mewe, Gronenschild & van den Oord 1985; Mewe, Lemen & van den Oord 1986; Kaastra 1992; Liedahl, Osterheld & Goldstein 1995), the EPIC data demand that the plasma possess a temperature of at least $kT \sim 50 \text{ keV}$ in order to reproduce the constraint on the hydrogen-like/helium-like equivalent width while simultaneously not curving the overall continuum excessively. The required emission measure would be $EM \equiv n^2 V = 1.6 \times 10^{67} \text{ cm}^{-3}$, where n is the electron number density and V is the volume of the thermal plasma. If we further suppose that this plasma surrounds the central engine in a spherical geometry which is optically-thin to Compton scattering (or else we would not observe rapid X-ray variability from the AGN), we can use the column density and emission measure constraints to conclude that the thermal plasma must have an extent of at least $4 \times 10^{16} \text{ cm}$. It is hard to understand the existence of such high temperature plasma many thousands

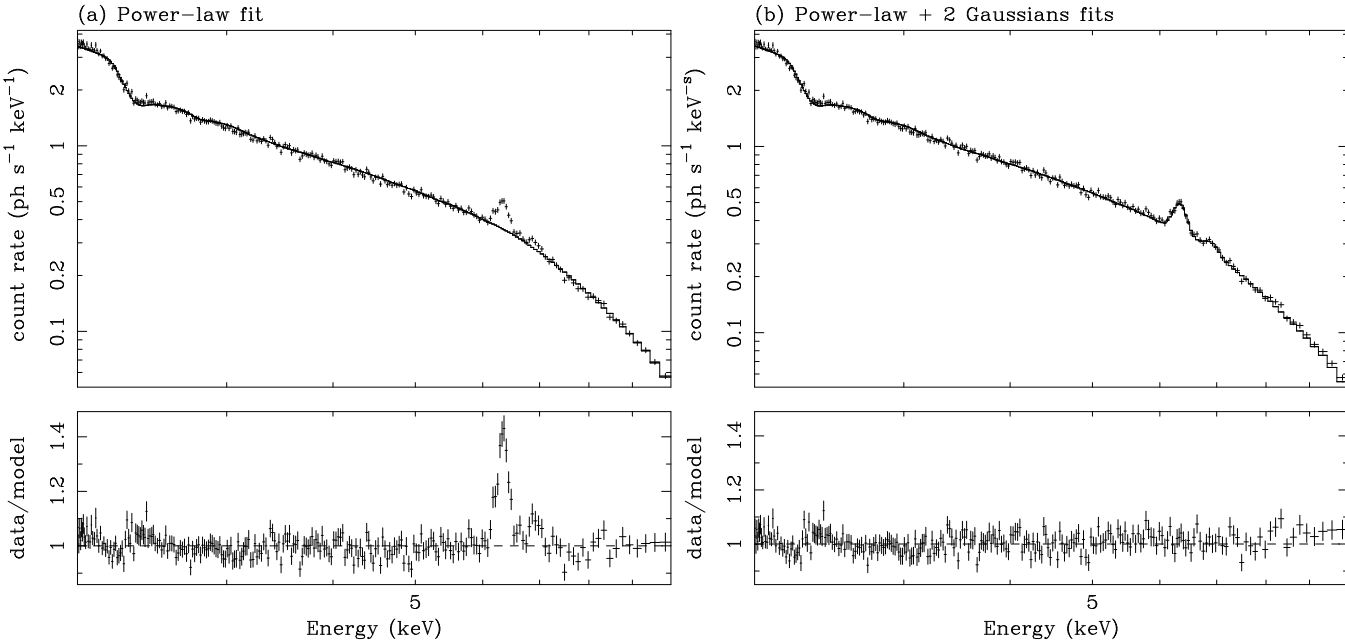


Figure 1. Spectral fits to the 2–10 keV EPIC-pn data from *XMM-Newton*. Panel (a) shows the fit with a model consisting of a simple power-law modified by the effects of Galactic absorption ($N_{\mathrm{H}} = 1.97 \times 10^{20} \mathrm{cm}^{-2}$). Two prominent emission lines are clearly visible in the lower ratio plot — one corresponds to the $\mathrm{K}\alpha$ line of cold iron (less than Fe XVII) while the other corresponds to the $\mathrm{K}\alpha$ line of hydrogen-like iron (Fe XXVI).

of gravitational radii from the black hole. Thus we disfavour this origin for the ionized iron line.

It is more likely that the ionized iron emission line originates via radiative recombination and resonant scattering in strongly photoionized gas within the central engine of the AGN. While a detailed exploration of this is beyond the scope of this paper, it is tempting to identify this feature with the same plasma that produces the highly ionized absorption features seen in several other AGN (Reeves, O’Brien & Ward 2003; Pounds et al. 2003).

3.2 Limits on a broad iron line

Is there evidence for a relativistically-broad iron line once the narrow lines have been modeled? To answer this question, we add a relativistic iron line to the spectral fit using two models to describe its profile; the Schwarzschild model of Fabian et al. (1989) as implemented in the `diskline` model of XSPEC package, and the near-extreme Kerr model of Laor (1991) as implemented in XSPEC’s `laor` model. The energy of the emission line, E_{broad} , was allowed to vary across the range of possible Fe $\mathrm{K}\alpha$ transition energies, 6.40 keV to 6.97 keV (rest-frame). The inner radius of the emitting region r_{in} , the emissivity index* of the disk β , the viewing inclination i , and the line normalization are also free parameters in the fit. The outer radius of the line emitting region was fixed at $r = 1000r_g$ (where $r_g = GM/c^2$). The improvement in the goodness of fit was $\Delta\chi^2 = 11$ and $\Delta\chi^2 = 10$ (for 5 additional degrees of freedom) for the `diskline` and

`laor` models, respectively. Such a change is *not* significant at the 90% level.

Thus, we have not obtained a detection of a broad iron emission line in the EPIC-pn spectrum of NGC 4593. In order to obtain a meaningful upper limit to the equivalent width of any broad iron line, we must specify its shape (since the data is incapable of doing that itself). We can proceed either empirically or theoretically. Empirically, we can assume that any such line has the “typical” profile found in co-added *ASCA* data by Nandra et al. (1997a), i.e., the `diskline` model with $E_{\mathrm{broad}} = 6.4 \mathrm{keV}$, $r_{\mathrm{in}} = 6r_g$, $\beta = 2.5$, $i = 29^\circ$. Using these assumptions, we can set an upper limit (with a 90% confidence level for one interesting parameter) to the broad line equivalent width of $W_{\mathrm{broad}} = 87 \mathrm{eV}$. Theoretically, the simplest model (Shakura & Sunyaev 1973; Novikov & Thorne 1974; Page & Thorne 1974) is one in which the accretion disk is geometrically-thin and radiatively-efficient, extends from the radius of marginal stability to large radii, and with an iron line emissivity that tracks the underlying dissipation (Reynolds & Nowak 2003; Reynolds et al. 2003). Applying such a line profile to the NGC 4593 data in the case of a near-extreme Kerr black hole (with dimensionless spin parameter $a = 0.998$) results in an upper limit to the equivalent width of 99 eV. These are significantly less than the values expected from theoretical reflection models ($\sim 200 \mathrm{eV}$ for solar abundances; e.g., Matt, Fabian & Reynolds 1997 and references therein) or observed in the Seyfert galaxy MCG-6-30-15 ($\sim 400 \mathrm{eV}$; Fabian et al. 2002). Thus, there appears to be a significant absence of spectral features from a relativistic accretion disk.

* The emissivity index is defined such that the emissivity of the line per unit proper area of the accretion disk is proportional to $r^{-\beta}$, where r is the Boyer-Lindquist radius.

4 WHERE ARE THE ACCRETION DISK SIGNATURES?

As discussed in the Introduction, the black hole accretion paradigm of AGN is very well established and supported by a significant body of evidence. Thus, the results of Section 3 beg us to turn the question around: why are we not seeing the X-ray reflection signatures of a relativistic accretion disk, given that we believe such a disk exists and is responsible for all of the AGN emissions that we observe? A straightforward solution to this problem would be to hypothesize sub-solar abundances of iron in the black hole accretion disk. If the light elements are present in cosmic abundance (Anders & Grevesse 1989), one needs iron to be under-abundant by a factor of 3 (i.e., $Z_{\text{Fe}} < 0.3$) in order to reduce the (cold) broad fluorescent emission below the 100 eV level as required by our data (e.g., see Reynolds, Fabian & Inoue 1995). If the light elements are *overabundant*, the enhanced photoelectric absorption further decreases the iron line equivalent width. A light element overabundance by a factor of two reduces the required iron underabundance to only 30% (i.e., $Z_{\text{Fe}} < 0.7$).

However, it would be surprising if the solution to the lack of a broad iron line was simply an underabundance of iron, given the highly evolved nature of stellar populations in the nuclei of galaxies such as NGC 4593. With this motivation, we explore modifications of the “canonical” line models discussed above and show that it is, in fact, rather easy to bury relativistic spectral features in the noise even if they are present at the level associated with cosmic abundance material.

4.1 Very broad lines and torqued accretion disks

Wilms et al. (2001) and Reynolds et al. (2004) have analyzed the EPIC-pn spectrum of MCG-6-30-15 in its Deep Minimum state and found it to possess *very* broadened X-ray reflection features. On the basis of these data, they suggest that the accretion disk in MCG-6-30-15 is being torqued by interactions with the central spinning black hole, producing a dissipation that is very centrally concentrated. By employing the disk models of Agol & Krolik (2001), Reynolds et al. (2004) suggest that the Deep Minimum state of MCG-6-30-15 corresponds to a torque-dominated (“infinite-efficiency”; see Agol & Krolik 2001) accretion disk viewed at an inclination of $30 - 40^\circ$.

There is little evidence for an obscuring molecular torus in MCG-6-30-15 (e.g., see Lee et al. 2002) and so, in principle, the central accretion disk could be viewed at any angle. It is interesting to note that if MCG-6-30-15 were observed at a high inclination with only moderate signal-to-noise, the Deep Minimum iron line would be so broad as to be undetectable against the noise of the continuum.

To explore whether this is also the case in NGC 4593, we add to the spectral fit a cold iron line with a profile corresponding to an infinite-efficiency accretion disk around a near-extreme Kerr black hole ($a = 0.998$). The inclination and normalization of the line were left as free parameters. This leads to only a slight improvement in the goodness of fit over the simple power-law plus narrow line model ($\Delta\chi^2 = 3$ for 2 additional degrees of freedom). Since this line is so broad, the upper limit on the equivalent width is $W_{\text{broad}} < 250$ eV. Thus, a broad line with the strength expected from

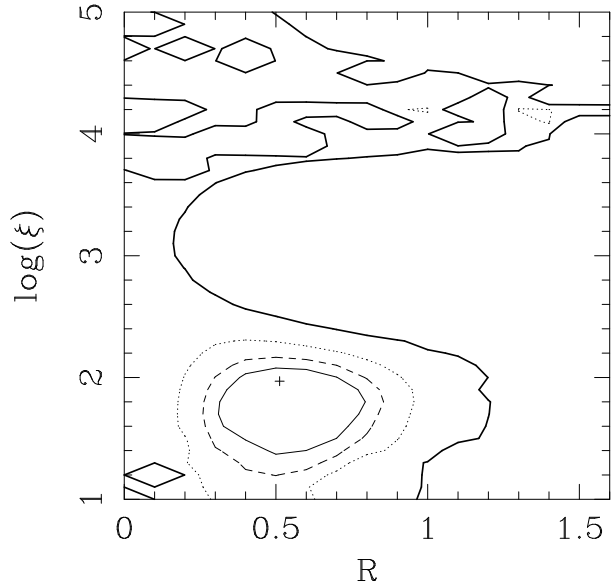


Figure 2. Confidence contours on the (ξ, R) -plane. Shown here are the 68% (thin solid line), 90% (dashed line) and 95% (dotted line) confidence contours using the best-fit ionized disk model (denoted by a cross). Also shown (thick solid line) is the contour corresponding to a goodness of fit parameter (χ^2) equal to the best fit power-law plus 2 narrow Gaussians. One can see that a “complete” disk (i.e. $R = 1$) is allowed if either moderately ionized disks ($\log \xi \sim 2$) or highly ionized disks ($\log \xi \sim 4$).

a cosmic abundance accretion disk is consistent with these data if the emissivity profile is very centrally concentrated.

4.2 Highly-ionized accretion disks

The prominence of X-ray reflection features can be significantly reduced by ionization of the accretion disk surface. Can ionization explain the lack of inner disk features in the spectrum of NGC 4593?

We address this question using the ionized reflection models of Ballantyne, Ross & Fabian (2001) convolved with the relativistic smearing model corresponding to a “standard” Novikov-Page-Thorne accretion disk around a near-extremal Kerr black hole. Figure 2 shows confidence contours on the (ξ, R) -plane, where ξ is the ionization parameter of the disk surface and R is the relative normalization of the disk reflection spectrum (defined such that an isotropic source above a plane-parallel reflector gives $R = 1$). Ionized disk reflection [with $\log(\xi) = 2, R = 0.5$] provides the best fit of any of the models reported in this paper ($\chi^2 = 1500/1470$) since it describes subtle concaved curvature that is actually present in the data. Using this as our reference fit, it can be seen that an almost complete disk (i.e. R almost unity) is possible provided the disk surface has an ionization parameter in the range $\log \xi = 1.5 - 2.5$. In this ionization range, the iron fluorescence line is strongly suppressed by resonant scattering followed by Auger destruction (Matt, Fabian & Ross 1993) thereby allowing the absence of a broad fluorescence line to be compatible with a complete disk. Using the slightly looser constraint that the ionized disk fit should be no worse than the no-disk fit (i.e., $\chi^2 < 1526$; thick contour on Fig. 2), we see that there is an additional “finger”

of allowed parameter space with $\log(\xi) \approx 4$, corresponding to highly ionized disks in which the iron atoms are mostly fully stripped.

Thus, in conclusion, even a standard Novikov-Payne-Thorne accretion disk is permissible in this object as long as it is either highly ionized (in which case the iron atoms are fully stripped) or moderately ionized (when the fluorescent line is strongly suppressed by resonant scattering and Auger destruction).

4.3 Limb-darkening and coronal attenuation from a high-inclination disk

As discussed in the Introduction, it is believed that any broad iron line is produced via fluorescence in the outer few Thomson depths of the optically-thick part of the black hole accretion disk. If viewed at high inclination (i.e., almost edge-on), there are two distinct “limb-darkening” effects that suppress the observed line flux (e.g., Reynolds, Maloney & Nowak 2000). Firstly, iron line photons can be photoelectrically absorbed on their passage through the outer layers of the disk, either by the K-shell edges of elements lighter than iron or the L-shell edges of iron. The resulting excited ion will then de-excite either via the Auger effect or through the emission of new fluorescent line photons. Either way, the result is a net loss of iron line photons from the observed spectrum. Secondly, iron line photons can be Compton scattered by energetic electrons in the X-ray emitting corona. If the corona can be described as a thermal plasma with temperature T , the average fractional energy shift per Compton scattering event is $\Delta E/E = 4kT/m_ec^2$, which is of the order of unity for typical coronal temperatures $kT \sim 100$ keV. Thus, Compton scattering effectively removes photons from the iron line, spreading them out in energy space into a broad pseudo-continuum.

Both of these effects, photoelectric absorption in the disk and Compton scattering in the corona, are strongly accentuated for high inclination observers since the photons then have to follow trajectories that graze the disk atmosphere and corona. The primary continuum photons, on the other hand, are not subject to limb-darkening since the corona is optically-thin. Hence, the equivalent width of a broad iron line would be expected to drop (possibly dramatically) as the disk is viewed increasingly edge-on. While there is little evidence (e.g., excess neutral absorption) that the inner disk of NGC 4593 is viewed at high-inclination, the possibility that limb-darkening is responsible for the absence of a broad line in this Seyfert nucleus cannot be ruled out with current data. If this is the correct explanation, a deeper observation might be able to uncover the limb-darkened broad iron line displaying a profile that has been modified by the effects of limb-darkening (Beckwith & Done 2004).

4.4 Other possibilities

Until now, we have been examining models of “complete” accretion disks, i.e., disks that remain geometrically-thin and radiatively-efficient from the radius of marginal stability to very large radii. In particular, we have been examining how extreme broadening or ionization can render a

reasonable strength iron line undetectable, even in a moderately long *XMM-Newton* observation. If one or both of these effects are responsible for the lack of an obvious broad line in NGC 4593, higher signal-to-noise spectroscopy either with a deeper *XMM-Newton* observation or (eventually) *Constellation-X* and *XEUS* will reveal the subtle signatures of the relativistically smeared reflection. However, it is also possible that the broad iron line is genuinely absent. There are two possible scenarios.

4.4.1 Advection dominated accretion disks

Firstly, the accretion disk may possess a transition point inside of which accretion switches to a hot, geometrically-thick, optically-thin mode. There has been extensive theoretical work on such flows (e.g., Ichimaru 1977; Rees 1982; Narayan & Yi 1994; Blandford & Begelman 1999; Narayan et al. 2002). Of relevance here are the class of flows that are advection-dominated (i.e., the locally-dissipated energy is not locally radiated) because of their low accretion rate. In terms of their iron-K band spectra, these disks would lack any very broad component, possessing a rather narrower iron line resulting from fluorescence of the thin-disk surface beyond the transition radius. The equivalent width of these features is determined by the solid angle that the thin-disk subtends at the X-ray source (which, in this scenario, would be thermal bremsstrahlung and Comptonization in the hot/geometrically-thick inner accretion flow). Although dependent on the precise geometry, these iron $K\alpha$ equivalent widths can be reduced from the plane-parallel case by factors of 2–4 (i.e. to 50–100 eV).

Indeed, it is possible that we are seeing just such a component in the form of the narrow 6.40 keV line modeled in Section 3. If we model this feature with a `diskline` profile possessing an inner truncation radius, instead of a narrow Gaussian profile, we determine that the inner truncation radius to the line emitting region is $r_{in} > 200r_g$. In deriving this number, we have fitted the `diskline` model assuming an emissivity index of $\beta = 3$ (appropriate for illumination of a flat disk by a central raised corona or advection dominated region), and a rest-frame line energy of 6.40 keV. The equivalent width of this feature is $W = 113 \pm 13$ eV with a goodness of fit of $\chi^2/\text{dof} = 1529/1470$; i.e., the truncated `diskline` profile produces very comparable results to the narrow Gaussian profile.

4.4.2 Strongly beamed primary emission

Secondly, it is possible that the observed X-ray continuum does not originate from, and does not irradiate, the accretion disk. The most likely alternative is that the X-ray continuum originates from a relativistic jet flowing from the inner regions; the primary X-rays are then beamed away from the accretion disk, and X-ray reflection from the disk is very strongly suppressed. Given the high amplitude variability seen on hour-timescales within this object, the X-rays would have to originate from the inner parts of any jet.

5 CONCLUSIONS

In this paper, we have analyzed the 2–10 keV *XMM-Newton* EPIC-pn spectrum of NGC 4593, with particular emphasis on the implications of this spectrum for the nature of the accretion flow in this Seyfert-1 nucleus. Only two spectral features are detected which can be identified with narrow K α emission lines of cold and hydrogen-like iron at 6.40 keV and 6.97 keV, respectively. Once these have been modelled, the spectrum has a power-law form (to within a 3–4% accuracy) across the 2–10 keV band.

We fail to detect any X-ray reflection features from a relativistic accretion disk. However, we show that, even if a radiatively-efficient geometrically-thin complete accretion disk exists, its X-ray reflection signatures would be buried in the noise if the accretion disk has either a very centrally concentrated irradiation profile or an appropriately ionized surface. Either of these models can be tested by longer EPIC observations which would be sensitive to the subtle features displayed by a highly blurred or ionized reflection spectrum. If longer observations still fail to detect any accretion disk signatures, we are forced to consider other scenarios. Firstly, the inner disk may be very hot and optically-thin, thereby being incapable of producing any X-ray reflection features. Secondly, the observed X-ray continuum might be highly anisotropic, being strong beamed away from the disk (and towards the observer) thereby rendering any disk features undetectable.

ACKNOWLEDGMENTS

We thank Andrew Young for stimulating discussion throughout the course of this work. We acknowledge support from the NASA/*XMM-Newton* Guest Observer Program under grant NAG5-10083, and the National Science Foundation under grant AST0205990.

REFERENCES

Agol E., Krolik J. H., 2000, ApJ, 528, 161
 Ballantyne D.R., Ross R.R., Fabian A.C., 2001, MNRAS, 327, 10
 Basko M.M., 1978, ApJ, 223, 268
 Blandford R.D., Begelman M.C., 1999, MNRAS, 303, L1
 Elvis M., Wilkes B.J., Lockman F.J., 1989, AJ, 97, 777
 Dewangan G.C., Griffiths R.E., Schurch N.J., 2003, ApJ, 592, 52
 Fabian A.C., Ress M.J., Stella L., White N.E., 1989, MNRAS, 238, 729
 Fabian A.C. et al., 2002, MNRAS, 331, L35
 George I.M., Fabian A.C., 1991, MNRAS, 249, 352
 Grupe D., Wills B.J., Leighly K.M., Meusinger H., 2004, AJ, 127, 156
 Guilbert P.W., Rees M.J., 1988, MNRAS, 233, 475
 Kaastra J.S., 1992, An X-ray Spectral Code for Optically-Thin Plasmas (Internal SRON-Leiden Report, updated version 2.0)
 Laor A., 1991, ApJ, 376, 90
 Lee J.C., Iwasawa K., Houck J.C., Fabian A.C., Marshall H.L., Canizares C.R., 2002, ApJ, 570, L47
 Liedahl D.A., Osterheld A.L., Goldstein W.H., 1995, ApJL, 438, 115
 Lightman A.P., White T.R., 1988, ApJ, 335, 57
 Matt G., Fabian A.C., Reynolds C.S., 1997, MNRAS, 289, 175
 Matt G., Perola G.C., Piro L., 1991, A&A, 245, 63
 Mewe R., Gronenschild E.H.B.M., van den Oord G.H.J., 1985, A&AS, 62, 197
 Mewe R., Lemen J.R., van den Oord G.H.J., 1986, A&AS, 65, 511
 Nandra K., George I.M., Mushotzky R.F., Turner T.J., Yaqoob T., 1997a, ApJ, 477, 602
 Nandra K., George I.M., Mushotzky R.F., Turner T.J., Yaqoob T., 1997b, ApJ, 476, 70
 Narayan R., Yi I., 1994, ApJ, 428, L13
 Narayan R., Quataert E., Igumenshchev I.V., Abramowicz M.A., 2002, ApJ, 577, 295
 Novikov I.D., Thorne K.S., in Black Holes, eds. C.DeWitt & D.DeWitt, 1974, pp.343.
 Page D.N., Thorne K.S., 1974, ApJ, 191, 499
 Pounds K.A., Reeves J.N., King A.R., Page K.L., O'Brien P.T., Turner M.J.L., 2003c, MNRAS, 345, 705
 Pounds K.A., Reeves J.N., Page K.L., Edelson R., Matt G., Perola G.C., 2003b, MNRAS, 341, 953
 Pounds K.A., Reeves J.N., Page K.L., Wynn G.A., O'Brien P.T., 2003a, MNRAS, 342, 1147
 Rees M. J., 1982, in Riegler G., Blandford R. D., eds, The Galactic Center, Am. Inst. Phys., New York, p.166.
 Reeves J.N., O'Brien P.T., Ward M.J., 2003, ApJ, 593, L65
 Reynolds C.S., Nowak M.A., 2003, Physics Reports, 377, 389
 Reynolds C.S., Nowak M.A., Maloney P.R., 2000, ApJ, 540, 143
 Reynolds C.S., Wilms J., Begelman M.C., Staubert R., Kendziorra E., 2003, MNRAS, in press
 Shakura N.I., Sunyaev R., 1973, A&A, 24, 337
 Tanaka, Y., et al., 1995, Nature, 375, 659
 Terashima Y., Iyomoto N., Ho L.C., Ptak A.F., 2002, ApJS, 139, 1
 Turner T.J., et al., 2002, ApJ, 574, L123
 Wilms J., Reynolds C.S., Begelman M.C., Reeves J., Molendi S., Staubert R., Kendziorra E., 2001, MNRAS, 328, L27